

Zeitschrift: Schweizerische mineralogische und petrographische Mitteilungen =
Bulletin suisse de minéralogie et pétrographie

Band: 83 (2003)

Heft: 1

Artikel: Ti-bearing andradite-prehnite-epidote assemblage from the Malá Fatra
granodiorite and tonalite (Western Carpathians)

Autor: Faryad, Shah Wali / Dianiška, Ivan

DOI: <https://doi.org/10.5169/seals-63134>

Nutzungsbedingungen

Die ETH-Bibliothek ist die Anbieterin der digitalisierten Zeitschriften auf E-Periodica. Sie besitzt keine Urheberrechte an den Zeitschriften und ist nicht verantwortlich für deren Inhalte. Die Rechte liegen in der Regel bei den Herausgebern beziehungsweise den externen Rechteinhabern. Das Veröffentlichen von Bildern in Print- und Online-Publikationen sowie auf Social Media-Kanälen oder Webseiten ist nur mit vorheriger Genehmigung der Rechteinhaber erlaubt. [Mehr erfahren](#)

Conditions d'utilisation

L'ETH Library est le fournisseur des revues numérisées. Elle ne détient aucun droit d'auteur sur les revues et n'est pas responsable de leur contenu. En règle générale, les droits sont détenus par les éditeurs ou les détenteurs de droits externes. La reproduction d'images dans des publications imprimées ou en ligne ainsi que sur des canaux de médias sociaux ou des sites web n'est autorisée qu'avec l'accord préalable des détenteurs des droits. [En savoir plus](#)

Terms of use

The ETH Library is the provider of the digitised journals. It does not own any copyrights to the journals and is not responsible for their content. The rights usually lie with the publishers or the external rights holders. Publishing images in print and online publications, as well as on social media channels or websites, is only permitted with the prior consent of the rights holders. [Find out more](#)

Download PDF: 09.12.2025

ETH-Bibliothek Zürich, E-Periodica, <https://www.e-periodica.ch>

Ti-bearing andradite–prehnite–epidote assemblage from the Malá Fatra granodiorite and tonalite (Western Carpathians)

Shah Wali Faryad¹ and Ivan Dianiška²

Abstract

Calc-silicate minerals (Ca-garnet, prehnite, epidote, titanite, actinolite) occur associated with chlorite and muscovite in Variscan tonalite and granodiorite of the Tatricum Unit in the Malá Fatra Mountains. They formed during post-magmatic cooling of granitoids. Garnet is rich in fluorine (F = 1.58 wt%) and Ti = 3.29 wt% with the end-member contents ranging between 50–74 mol% for andradite, 32–42% for grossularite and 1–14% for schorlomite + morimotoite. Major element contents in garnet indicate the exchanges of $\text{Fe}^{3+}\text{Al}_1$, $\text{Fe}^{2+}\text{TiFe}^{3+}_{-2}$ and $\text{VI Ti}^{\text{IV}}\text{Fe}^{3+\text{IV}}\text{Si}_{-1}\text{Al}_1$. Mineral assemblages and thermodynamic calculation indicate temperature of ca 360–380 °C at 0.2 GPa for garnet, prehnite and epidote formation. The tonalite and granodiorite were affected by Alpine metamorphic overprint, which resulted in deformation and formation of very low-grade mineral assemblages, involving pumpellyite, epidote, chlorite, muscovite, albite and microcline. P-T calculations yielded pressure of ca. 0.3 GPa at 300 °C for this metamorphic event in the Malá Fatra Mts. of the Tatricum Unit.

Keywords: Ti-bearing andradite, granitoids, hydrothermal alteration, Alpine metamorphism.

1. Introduction

Grossularite-andradite garnet with epidote, pumpellyite and prehnite occur in very low-grade metamorphic and hydrothermally altered rocks (Coombs et al., 1977; Tulloch, 1979; Cho and Liou, 1987). Ti-bearing andradite “melanite” contains high schorlomite, $\text{Ca}_3\text{Ti}_2\text{Fe}^{3+}_2\text{SiO}_{12}$, (e.g. Howie and Woolley, 1968; Kühberger et al., 1989) or morimotoite, $\text{Ca}_3\text{Fe}^{2+}\text{Ti}^{4+}\text{Si}_3\text{O}_{12}$, (Henmi et al., 1995) component that is a result of two different substitution mechanisms in the tetrahedral site. One type of titanian andradite can be interpreted as solid solution between morimotoite and andradite $\text{Ca}_3\text{Fe}^{2+}_2\text{Si}_3\text{O}_{12}$ with an additional substantial hydroandradite substitution (Lager et al., 1989; Armbruster et al., 1998). The other type of substitution that leads to schorlomite is $(\text{Fe}^{3+}, \text{Fe}^{2+}, \text{Ti}^{4+}, \text{Al}) \rightarrow \text{Si}^{4+}$ for which charge balance is achieved by Ti^{4+} in the octahedral site (Henmi, 1995; Armbruster et al., 1998). Most of these garnets exhibit a Si deficit charge balanced by the $(\text{O}_4\text{H}_4)^{4-} \rightarrow (\text{SiO}_4)^{4-}$ substitution.

Ti- and F-bearing Ca-grandite is found in association with epidote, pumpellyite, prehnite, titanite and muscovite in Variscan granodiorite, tonalite and in migmatite enclaves in tonalite in the Malá Fatra Mountains. Detailed petrographical

study of granitoids indicated various degree of deformation and very low-grade metamorphism that make difficult to distinguish minerals formed by these two processes. By analogy with other Western Carpathian units, this metamorphism is related to Cretaceous nappe tectonics and collisional processes that reached greenschist to epidote amphibolite facies conditions in the Veporicum unit (Fig. 1A), but for the Malá Fatra Mountains has not been known. The aims of the present study are: (1) to define mineral assemblages formed during post-magmatic hydrothermal alteration and those related to Alpine metamorphic overprint, (2) to analyze the compositional variations and the main substitutions in Ti-bearing Ca-grandite and (3) to specify temperature and pressure conditions for Alpine metamorphism.

2. Sample description

The grandite-bearing granodiorite and tonalite are part of the Tatricum basement rocks, which are exposed in the Malá Fatra Mountains in the northwestern part of the Slovak Republic (Fig. 1). The basement rocks include amphibolite-facies gneisses and amphibolites, migmatites and granitoids. The migmatites occur mainly along the

¹ Institute of Petrology and Structural Geology, Charles University, Albertov 6, 12843 Prague 2, Czech Republic. <faryad@natur.cuni.cz>

² Mierová 16, Roznava, Slovakia.

Table 1 Major element composition (wt%) of tonalite (average from 8 samples).

SiO ₂	Al ₂ O ₃	TiO ₂	Fe ₂ O ₃	MnO	MgO	CaO	Na ₂ O	K ₂ O	P ₂ O ₅	S	LOI
66.76	15.75	0.45	3.43	0.07	1.35	2.83	4.26	2.67	0.19	0.15	2.09

Total Fe as Fe₂O₃.

Table 2 Succession of mineral formation in the Malá Fatra granodiorite and tonalite.

Igneous phases	post-magmatic cooling	metamorphic overprint
Plagioclase	Garnet	Zeolite
K-feldspar	Epidote	Pumpellyite
Biotite	Prehnite	Microcline
Quartz	Muscovite	Epidote
Amphibole	Chlorite	Muscovite
Allanite	Titanite	Chlorite
	Albite	Calcite
	Microcline	Albite
	Quartz	Quartz
	Actinolite	

Table 3 Selected microprobe analyses of igneous biotite, plagioclase and amphibole from tonalite.

Sample Mineral	2005 Biotite	MHV565 Plagioclase	MHV565 Amphibole
SiO ₂	37.84	61.14	44.39
TiO ₂	3.40	0.06	0.84
Al ₂ O ₃	16.28	24.17	10.13
FeO	19.28	0.41	15.97
MnO	0.31	0.00	0.70
MgO	10.46	0.00	11.56
CaO	0.07	6.27	11.92
Na ₂ O	0.12	7.24	1.45
K ₂ O	9.81	0.36	1.07
Total	97.56	99.74	98.03

Formulae	per 11(O)*	8(O)	23 (O)**
Si	2.900	2.747	6.545
Ti	0.197	0.002	0.093
Al	1.470	1.280	1.760
Fe ³⁺	0.000	0.000	0.588
Fe ²⁺	1.236	0.018	1.381
Mn	0.021	0.000	0.087
Mg	1.195	0.000	2.541
Ca	0.006	0.302	1.883
Na	0.018	0.631	0.415
K	0.959	0.020	0.201
An		0.317	
Ab		0.652	
Or		0.020	

* 11 oxygens and 6 cations + Na + K + Ca.

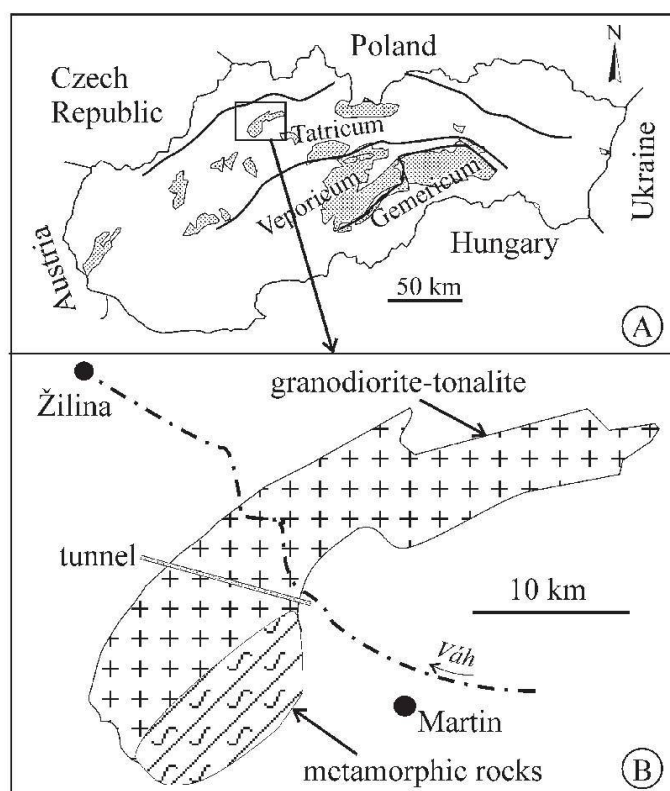
** Averaged Fe³⁺ from 13 and 15 cations.

Fig. 1 Distribution of the Pre-Alpine basement units in the Western Carpathians (A), Geological sketch map of the Malá Fatra basement unit (B) with location of the tunnel.

boundary of granitoid and metamorphic rocks, but also form enclaves (up to several meters in diameter) in the tonalite (Kamenecký et al., 1987). Thermobarometric data indicated peak P–T conditions of ca 700–750 °C/0.6 GPa for metapelitic migmatites and 700–750 °C/0.8–1.0 GPa for metabasites that occur in the contact zone with granitoids (Janák and Lupták, 1997). According to Bro-

ska et al. (1992) and Petřík et al. (1994), the granitoids belong to an I-type igneous suite that originated by dehydration melting of lower crust material and by underplated mantle magmas. Broska et al. (1997) estimated using Al content in hornblende a pressure of 0.32 GPa at 750–800 °C for crystallization of the granitoid. Variscan age of 360 ± 10 Ma of this intrusive complex was obtained by U–Pb (zircon) and Rb–Sr (whole rock) geochronological data (Bagdasaryan et al., 1992). The samples studied here are from the tonalite, granodiorite and its migmatite enclaves exposed in an exploration adit of the highway tunnel (Fig. 1B). Whole-rock chemical analyses of the tonalite are listed in Table 1.

The Malá Fatra granodiorite and tonalite are medium-grained, locally porphyritic with plagioclase and perthitic K-feldspar crystals. They indicate various degrees of alteration and deformation. Textural relations and mineral compositions indicate that minerals observed were formed by

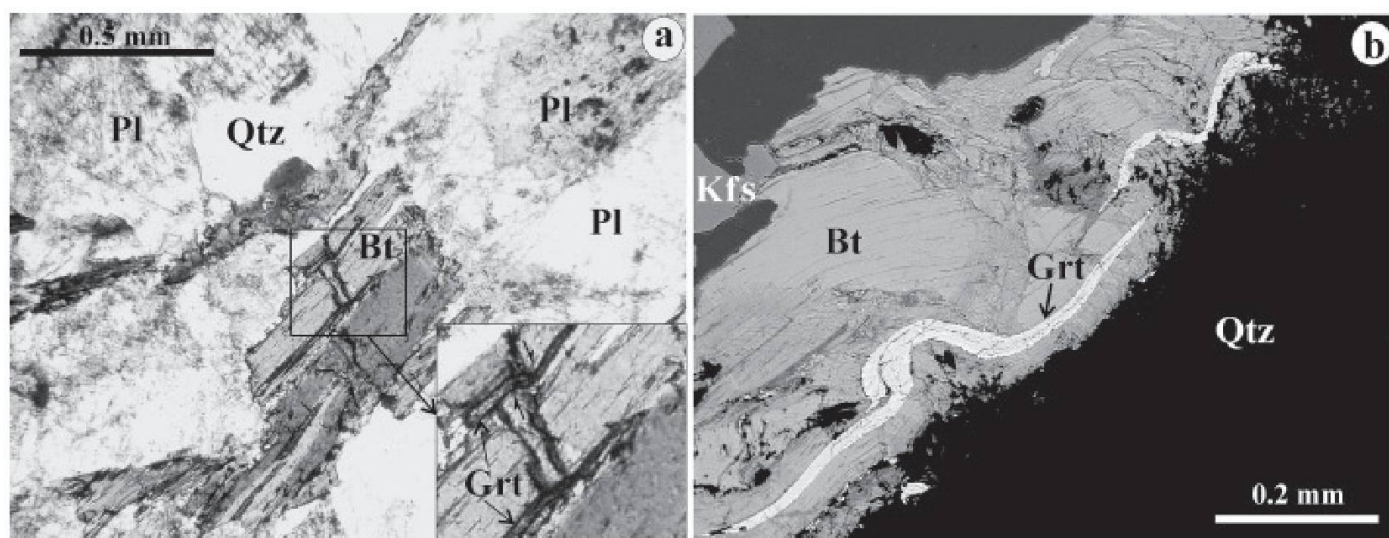


Fig. 2 Tonalite with saussuritized plagioclase, biotite and quartz. Trails of garnet along biotite cleavage are kinked (a) and folded (b). Note that garnet in (a) occurs only along cleavage.

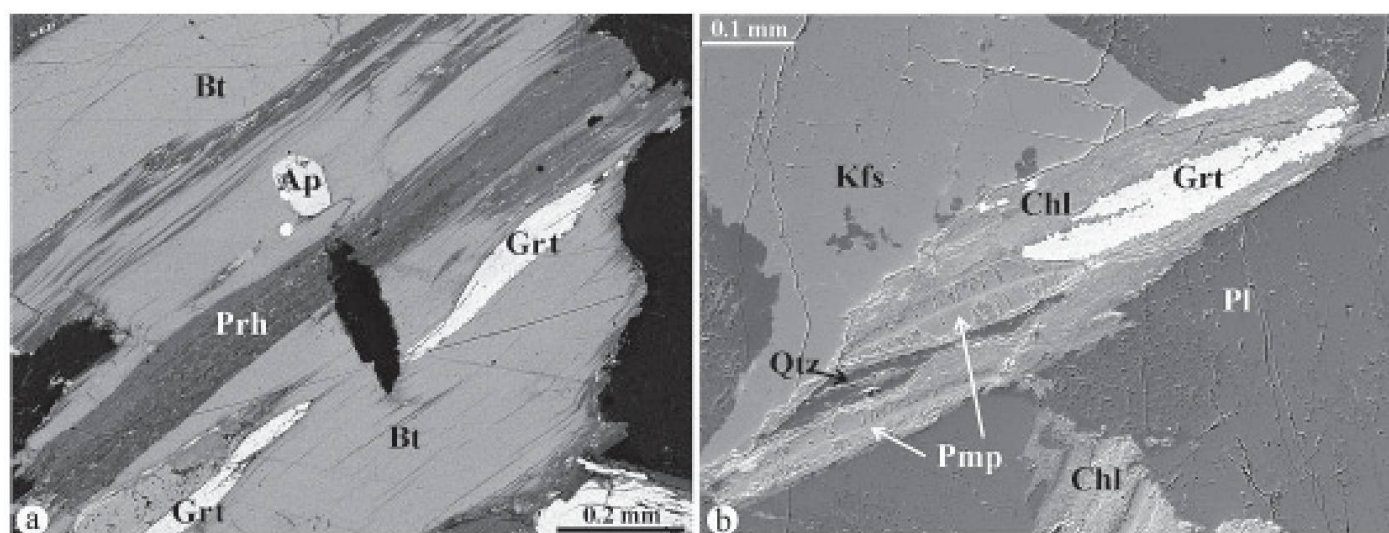


Fig. 3 Back-scattered electron images of stripes or lenses of garnet (Grt) and prehnite (Prh) in biotite (Bt) (a) and of garnet and pumpellyite (Pmp) in chlorite (Chl) (b) from a tonalite in the Malá Fatra Mts.

three different processes: (1) igneous, (2) post-magmatic hydrothermal and (3) metamorphic (Table 2). Point-counting of the granodiorite and tonalite yielded 43–62 vol% plagioclase, 17–33% quartz, 7–19% biotite and 0–25% K-feldspar. Accessory dark green amphibole, zircon, apatite and allanite with euhedral rim of epidote also belong to igneous phases in the rocks. Plagioclase may form inclusions in K-feldspar and it is usually replaced by fine-grained white mica and epidote, especially in the more calcic cores (Fig. 2). The migmatite displays a gneissic texture and consists mostly of plagioclase, quartz, K-feldspar and biotite. Biotite is altered to chlorite and locally contains epidote, titanite, garnet, prehnite and pumpellyite (Fig. 3).

Excepting strongly altered zones, the post-magmatic minerals (Table 2) are present in acces-

sory amounts. Garnet is present in most samples and in addition to chlorite and epidote it occurs adjacent to biotite, titanite, prehnite and locally to microcline. In most cases garnet forms thin strips, lenses, pods (0.1–0.6 mm in length) or bulbous grains of nearly colorless or pale brown color. Garnet is slightly anisotropic and its elongate crystals follow cleavage in biotite. In some cases the garnet trails in biotite are deformed (Fig. 2). Garnet, prehnite, pumpellyite and epidote can be observed in the same thin-section, even in the same chloritized biotite (Fig. 3). However prehnite, pumpellyite and epidote can be found also in plagioclase. Prehnite occurs in partly chloritized biotite but it was never found in biotite that was totally replaced by chlorite. Accessory hornblende is partly replaced by chlorite, epidote, titanite and actinolite.

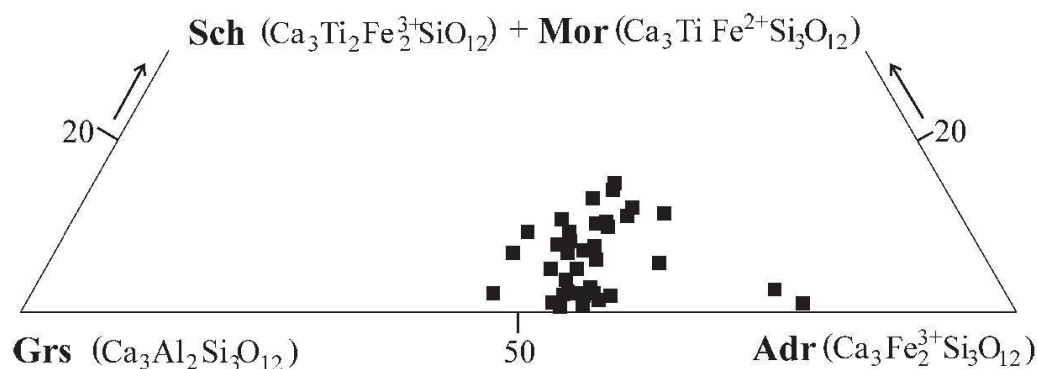


Fig. 4 Composition of Ti-bearing andradite from tonalite, granodiorite and migmatite samples displayed in a grossularite-andradite-(schorlomite + morimotoite) plot.

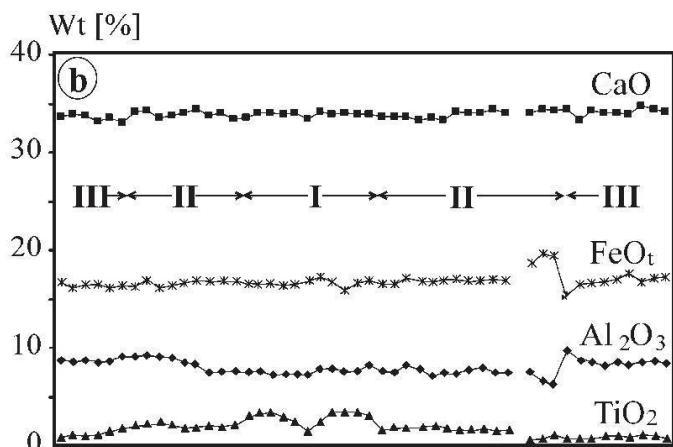
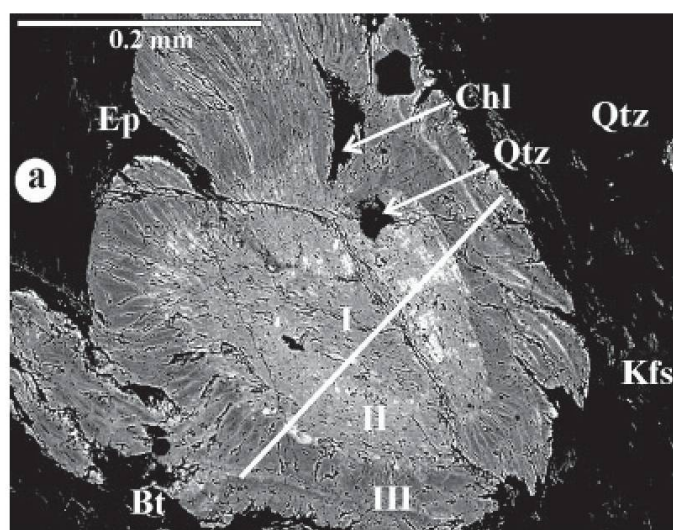


Fig. 5 Zoned grandite garnet (a) with compositional profiles of CaO, FeO, Al_2O_3 and TiO_2 (b). I–III indicate three compositional zones in garnet. Abbreviations: Bt—biotite, Chl—chlorite, Ep—epidote, Kfs—K-feldspar and Qtz—quartz. The brighter areas correspond to andradite-rich garnet and inclusions of Fe-oxide.

Granodiorite and tonalite reveal various degrees of deformation. Quartz shows undulatory extinction and large feldspar crystals form clasts with cracks filled with white mica and epidote. Strongly mylonitized tonalite and granodiorite consist of plastically deformed quartz, phengite

Table 4 Selected microprobe analyses of garnet from the Malá Fatra tonalite and granodiorite.

Sample	PMF-12	PMF-9	MHV-565		2199	2005
SiO ₂	36.23	35.98	35.68	35.50	34.811	35.68
TiO ₂	0.22	0.23	2.29	0.48	3.29	2.02
Al ₂ O ₃	8.97	11.09	10.14	10.84	6.84	9.87
Fe ₂ O ₃	18.42	14.82	14.40	15.81	18.81	16.50
FeO	0.00	0.91	1.42	0.61	0.47	1.41
MnO	0.43	0.45	0.36	0.51	0.40	0.30
MgO	0.02	0.04	0.19	0.04	0.15	0.00
CaO	34.47	35.45	35.08	34.77	34.74	33.21
F	0.48	1.11	0.74	1.58	—	—
Cl	0.01	0.03	0.00	0.01	—	—
Total	99.29	100.12	100.34	100.14	99.52	98.99
Atoms per formula unit (for normalization see text)						
Si	2.962	2.915	2.876	2.895	2.860	2.903
Ti	0.013	0.014	0.139	0.029	0.203	0.125
Al	0.856	1.032	0.962	1.038	0.662	0.959
Fe ³⁺	1.122	0.873	0.823	0.962	1.173	1.102
Fe ²⁺	0.000	0.063	0.138	0.043	0.021	0.110
Mn	0.029	0.030	0.025	0.035	0.028	0.021
Mg	0.003	0.004	0.023	0.005	0.018	0.000
Ca	2.990	2.997	3.027	3.028	3.055	2.934
Na	0.000	0.000	0.000	0.000	0.000	0.000
K	0.000	0.000	0.000	0.000	0.000	0.000
H	0.022	0.000	0.000	0.000	0.099	0.385
F	0.124	0.277	0.189	0.406	—	—
Cl	0.001	0.005	0.000	0.001	—	—
sps	1.0	1.0	0.9	1.2	1.0	0.7
alm	0.0	2.1	4.8	1.4	0.7	9.0
py	0.1	0.1	0.8	0.2	0.6	0.0
grs	41.9	49.2	43.7	48.5	32.0	39.7
sch	0.7	0.7	7.2	1.4	10.5	6.4
adr	56.4	46.8	42.6	47.4	55.1	44.1

–: not detected.

and albite. Besides epidote and/or white mica occurring in chloritized biotite (1) or in plagioclase (2), they are present also in shear cracks (3). In one case epidote overgrowing and rimming garnet was found. Veinlets of microcline are also present in the rocks. Up to 3 mm long zeolite crys-

tals were found in drusy vein occurring in a tectonic zone, which crosses the tonalite. Textural relations, mainly pumpellyite overgrowing prehnite, indicate formation of pumpellyite during progressive metamorphism after prehnite. Prehnite seems to be a metastable phase coexisting with pumpellyite. Pumpellyite replacing amphibole was also found. Calcite forms microveins in plagioclase and together with chlorite replaces amphibole.

3. Mineral Composition

Most minerals were analysed with a scanning electron microscope JEOL 6310 at the Institute for Mineralogy and Petrology in Graz equipped with wavelength- and energy-dispersive spectrometers. Some minerals were additionally analysed by Cameca SX 100 at the Geological Institute of Dionýz Štúr in Bratislava. Standards were pyrope (Mg, Al), adularia (K), rutile (Ti), tephroite (Mn), jadeite (Na, Si) and andradite (Fe, Ca). Operating conditions were 15 kV, 10 or 15 nA with 20 s counting time. Representative mineral analyses are given in Tables 3–6.

In the tonalite and granodiorite, the igneous phases are biotite ($X_{Mg} = 0.37–0.49$, $Ti = 0.4$ a.p.f.u.), plagioclase ($An_{14–33}$), K-feldspar edenitic amphibole ($Si = 6.54$ a.p.f.u., $X_{Mg} = 0.64$, Table 3).

Biotite in the migmatite is rich in Ti (0.53 a.p.f.u.) and has $X_{Mg} = 0.39$. The anorthite contents in plagioclase from the migmatite range between An_{22} and An_{29} . K-feldspar has near end-member composition ($Na < 0.06$ a.p.f.u.).

Microprobe analyses of garnet indicate up to 3.29 wt% TiO_2 and 1.58 wt% F (Table 4). The mineral formulae of garnet, calculated by combination of hydrogarnet and schorlomite substitutions, can be written as $(Ca, Fe^{2+})_3(Al, Fe^{3+}, Ti^{4+})_2(Si, Fe^{3+}O_4)_{3-x}(OH, F)_{4x}$. The value of H_4Si^- is usually set by the charge deficiency that we have balanced hydroxyl substitution. According to Amthauer and Rossman (1998) this substitution, investigated using Fourier transform IR spectroscopy, occurs by the exchange of $(SiO_4)^{4-} = (O_4H_4)^{4-}$. Samples with analytical totals equal to 100 suggest that the hydroxyl group $[(OH, F)_4]^{4-}$ is occupied only by F (Table 4). In samples with low analytical totals and low TiO_2 contents, the hydrogarnet substitution was normalized to $(Ca+Fe+Ti+Al+Mg+Mn) = 5$. Most analyses indicate maximum hydroxyl content $x = (OH, F)/4 = 0.1$ a.p.f.u. in garnet. This value was used also for schorlomite substitution in Ti-rich garnet, where the analyses were normalized to $(Ca+Fe+Ti+Al+Mg+Mn+Si) = 8+x$.

The garnet composition varies in the range of 22–44 mol% grossularite, 46–74% andradite,

Table 5 Microprobe analyses of epidote, prehnite and pumpellyite from tonalite.

Mineral	Epidote			Prehnite			Pumpellyite	
Sample	2005	2199		2005	2199		2199	
Position		in Pl		in Pl	in Bt			
SiO ₂	36.49	36.79	37.42	43.58	43.17	43.070	37.27	38.08
TiO ₂	0.12	0.13	0.00	0.00	0.06	0.090	0.18	0.01
Al ₂ O ₃	20.80	20.55	22.19	23.11	21.18	18.510	20.19	23.75
Fe ₂ O ₃	15.35	16.04	12.90	1.29	3.678	8.42	8.238	3.828
FeO	–	–	–	–	–	–	3.248	1.251
MnO	0.61	0.80	0.00	0.55	0.07	0.00	0.08	0.17
MgO	0.11	0.00	0.06	0.07	0.00	0.00	2.71	3.93
CaO	21.73	21.09	21.87	26.28	26.97	25.35	22.67	22.99
Total	95.21	95.4	94.44	94.88	95.128	95.44	94.59	94.01
Formulae per	12.5 (O)			11 (O)				
Si	3.019	3.046	3.077	3.025	3.025	3.056	6.049	6.051
Ti	0.007	0.008	0.000	0.000	0.003	0.005	0.022	0.001
Al	2.028	2.005	2.150	1.890	1.749	1.548	3.861	4.448
Fe ³⁺	0.959	1.011	0.803	0.0749	0.1939	0.461	1.006	0.458
Fe ²⁺	–	–	–	–	–	–	0.441	0.166
Mn	0.042	0.056	0.000	0.032	0.004	0.000	0.011	0.023
Mg	0.014	0.000	0.007	0.007	0.000	0.000	0.657	0.931
Ca	1.926	1.871	1.927	1.954	2.025	1.927	3.942	3.914
Zo	0.03	0.01	0.17					
Ep	0.97	0.99	0.83					
X _{Fe} ³⁺	0.321	0.335	0.272	0.034	0.099	0.230	0.207	0.093

Atoms per formula unit: epidote (12 oxygens + 1 OH), prehnite (11 oxygens and 7 cations), pumpellyite (49 oxygens and 16 cations).

Table 6 Microprobe analyses of white mica, chlorite, actinolite and K-feldspars from tonalite.

Sample	2005				MHV565		
Mineral	Muscovite				Chlorite	Kfs	Act
Position	in vein	in Pl	shear cracks		with Grt	in Chl	rim of Ed
SiO ₂	44.74	44.92	47.69	48.01	29.55	63.45	54.42
TiO ₂	1.11	0.71	0.76	0.55	0.11	0.29	0.05
Al ₂ O ₃	26.65	28.47	29.14	29.66	16.40	18.04	1.1
FeO	6.63	6.71	5.72	4.98	23.04	0.39	13.16
MnO	0.63	0.63	0.01	0.08	0.92	0.00	0.76
MgO	1.58	1.21	1.70	1.14	18.21	0.05	15.41
CaO	0.10	0.04	0.00	0.00	0.24	0.04	12.46
Na ₂ O	0.20	0.27	0.12	0.00	0.01	0.69	0.4
K ₂ O	9.45	9.48	10.06	9.99	0.02	15.49	0.05
Total	91.35	92.64	95.20	94.41	88.50	98.44	97.82
Formulae per	11(O)*				28(O)	8(O)	23(O)
Si	3.197	3.159	3.242	3.293	6.128	2.980	7.827
Ti	0.060	0.038	0.039	0.029	0.017	0.010	0.005
Al	2.244	2.359	2.334	2.398	4.008	0.999	0.186
Fe ³⁺	0.000	0.000	0.000	0.000	0.000	0.000	0.1897
Fe ²⁺	0.393	0.380	0.325	0.286	3.995	0.014	1.3931
Mn	0.038	0.038	0.001	0.005	0.161	0.000	0.093
Mg	0.169	0.127	0.173	0.117	5.629	0.003	3.304
Ca	0.008	0.004	0.000	0.000	0.052	0.002	1.920
Na	0.028	0.037	0.016	0.000	0.002	0.063	0.112
K	0.861	0.851	0.872	0.874	0.006	0.928	0.009

* 11 oxygens and 6 cations + Na + K + Ca.

Kfs: K-feldspar, Act: actinolite, Ed: edenite.

1–10% schorlomite, 0–5% morimotoite (Fig. 4), 0.5–2.5% spessartine, 0–1% pyrope, 0.0–3.5 almandine. Some isometric garnet grains exhibit irregular zoning, but generally cores are Ti-rich and rims grossular-rich (I–III, Fig. 5), where cores are relatively rich in Ti and rims have higher Al contents. The lighter domains and narrow bands in Fig. 5a correspond to Fe-rich and Ti-poor garnet with up to 74 mol% andradite content.

To trace compositional changes and Ti variation in garnet, the model of additive components of grossularite (Labotka, 1995) and andradite (Russell et al., 1999) with some exchange components: $\text{Al}[\text{Fe}^{3+}]_{-1}$, H_4Si_{-1} , TiSi_{-1} , FeAl_{-1} , FeCa_{-1} , Mg-TiAl_{-2} , $\text{Fe}^{2+}\text{Mg}_{-1}$, MnCa_{-1} , MgCa_{-1} , $\text{TiMg}[\text{Fe}^{3+}]_{-2}$ and $(\text{TiFe}^{3+}\text{Si}_{-1}\text{Al}_{-1})$ can be adopted. Because of very small amounts of Mn and Mg in the studied garnet, the last five exchange components are neglected.

The most significant correlation occurs among the components TiSi_{-1} , $\text{Fe}^{3+}\text{Al}_{-1}$, indicating decrease of Al and Si in Ti-rich garnet compared to that in Ti-poor garnet. The TiSi_{-1} ($\text{TiFe}^{3+}\text{Si}_{-1}\text{Al}_{-1}$) exchange to andradite defines schorlomite ($\text{Ca}_3\text{Ti}_2\text{Fe}_2^{3+}\text{SiO}_{12}$), and morimotoite ($\text{Ca}_3\text{Fe}^{2+}\text{Ti}^{4+}\text{Si}_3\text{O}_{12}$) is described by applying one unit of $\text{TiFe}^{2+}[\text{Fe}^{3+}]_{-2}$ exchange to andradite (Fig. 6).

Epidote is rich in Fe^{3+} with very small clinozoisite contents of 0.01–0.17 (Table 5). Higher clinozoisite content shows epidote located in plagioclase. The $\text{Fe}^{3+}/(\text{Al}+\text{Fe}^{3+})$ values in most prehnite occurring in biotite and chlorite are around 0.1, but low-Fe prehnite with a value of 0.03 is present in plagioclase. Iron-rich prehnite with $X_{\text{Fe}^{3+}} = 0.23$ was analyzed in biotite (Table 5). The chemical formula of pumpellyite was calculated using the general formula $\text{W}_4 \text{X} \text{Y}_5 \text{Z}_6 \text{O}_{(20+x)} \text{OH}_{(8-x)}$, where $\text{W} = \text{Ca}, \text{Na}$, $\text{X} = \text{Fe}, \text{Mg}, \text{Mn}$, $\text{Y} = \text{Fe}^{3+}, \text{Al}, \text{Cr}, \text{Ti}$ and $\text{Z} = \text{Si}$ (Coombs et al. 1976). It shows slight variation in MgO (2.5–4.5 wt%) and major variation in Al_2O_3 (16.6–23.8 wt%) and Fe_2O_3 (4.5–15.5 wt%) contents (Fig. 7). Most pumpellyite grains are zoned with increase of Al (3.86–4.448 a.p.f.u.) and Mg (0.66–0.93 a.p.f.u.) and decrease of $\text{Fe}^{3+}_{\text{tot}}$ (1.44–0.61 a.p.f.u.) from core to rim.

There is no systematic compositional change between different textural varieties of white mica and chlorite. The Si values of phengite are in the range of 3.15–3.29 a.p.f.u. based on 11 oxygens (Table 6). Chlorite has $X_{\text{Mg}} = 0.58$. Microcline forms thin veinlets in the rock. Accessory actinolite rimming or overgrowing edenite has Si = 7.6–7.9, $\text{Al}_{\text{tot}} = 0.2–0.4$ a.p.f.u. and $X_{\text{Mg}} = 0.7$.

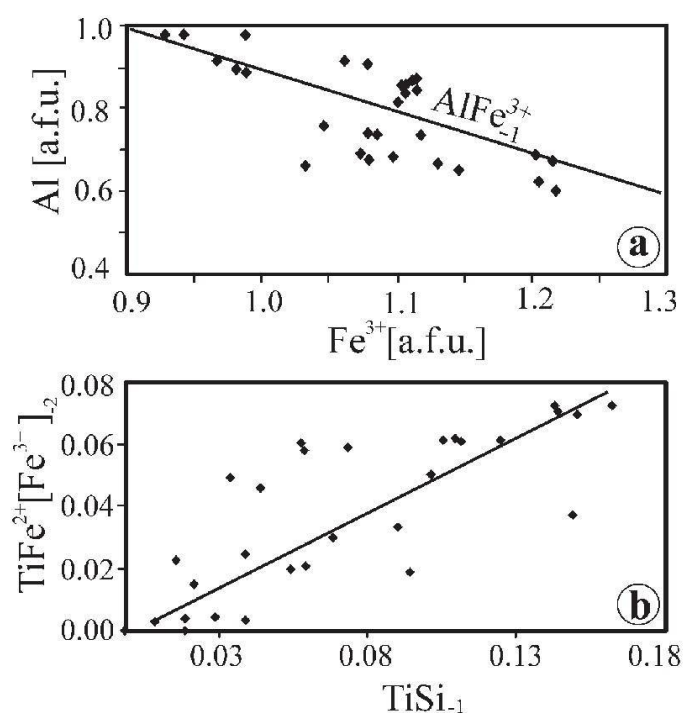


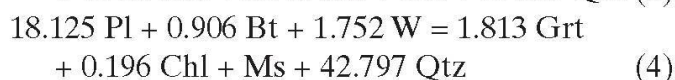
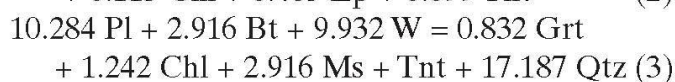
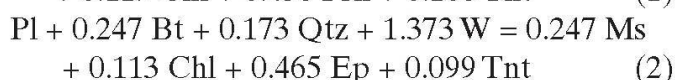
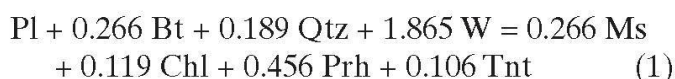
Fig. 6 Compositional variation in titanian grandite garnet from the Malá Fatra Mts. are summarized in plots of $\text{Al}:\text{Fe}^{3+}$ (a) and $\text{TiFe}^{2+}[\text{Fe}^{3+}]_2$ vs. TiSi_1 (b). The exchange component $\text{TiFe}^{2+}[\text{Fe}^{3+}]_2$ results from combining the two exchange vectors $\text{TiMg}^{2+}[\text{Fe}^{3+}]_2$ and FeMg_1 (Russell et al., 1999).

4. Origin and P–T conditions of metamorphic minerals

Mineral assemblages consisting of grandite, prehnite and epidote have been widely reported from very low-grade metamorphic rocks and from intrusive complexes, where they are result from hydrothermal convection systems during cooling of igneous rocks. Freiburger et al. (2001) assumed that hydrogarnet in plutonic rocks from the NW Massif Central (France) represents an early post-magmatic phase, predating prehnite. This interpretation can be adopted for garnet and coexisting prehnite, epidote, titanite and chlorite, replacing biotite in the Malá Fatra rocks. The presence of deformed and kinked garnet along biotite cleavage (Fig. 2) is a good argument for formation of garnet prior to deformation and very low-grade metamorphism. However, rims of some zoned garnets with relatively low Ti and high Al (Fig. 5) could be related to a later metamorphic process. Other minerals related to the cooling history of granitic magma are actinolite replacing edenite and microcline occurring in biotite with prehnite and garnet. Muscovite formed during this event occurs within or adjacent to chloritized biotite.

The replacement of biotite by chlorite releases Ti, K and some Si in exchange for H_2O (e.g. Leake, 1998; Russell et al., 1999). Ca necessary for

garnet, epidote, prehnite and titanite must have been obtained largely from the altered calcic cores of the plagioclase. Potassium released from biotite was incorporated in muscovite while Ti played an essential role in formation of titanite and schorlomite and morimotoite components in garnet. Mass balance between reactants and products, involving Ti-rich core of garnet, can be estimated based on the chemical composition of minerals involved in the hydrothermal or metamorphic system. Replacement of biotite through prehnite or epidote in the grandite-absent reactions led to the formation of titanite:



These reactions were calculated for average composition of minerals given in Table 3–6 and Ti-rich grandite with maximum Ti = 0.203 a.p.f.u. All reactions producing secondary minerals occurred by the supply of fluids.

To estimate P–T conditions of crystallization of tonalite and granodiorite, the amphibole-plagioclase thermobarometry, using the software program by Anderson (1996), was applied. The es-

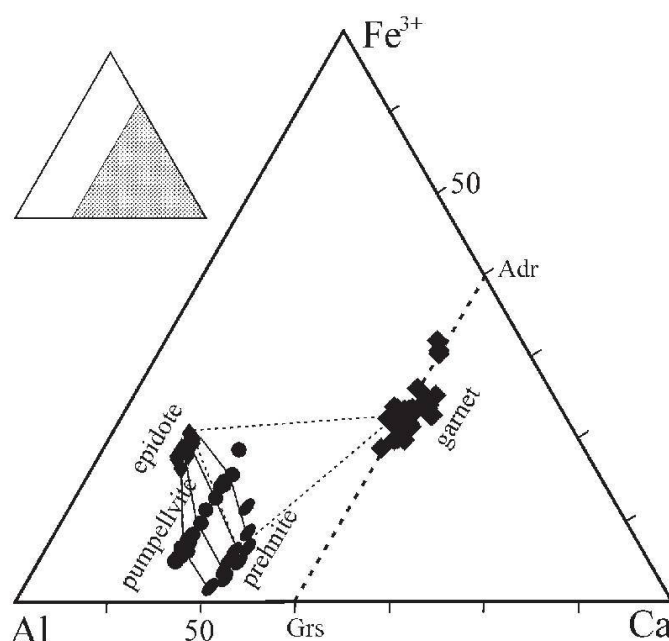


Fig. 7 Al– Fe^{3+} –Ca diagram showing the variation of garnet, prehnite, pumpellyite and epidote. Dashed and solid lines connect post-magmatic and metamorphic phases respectively.

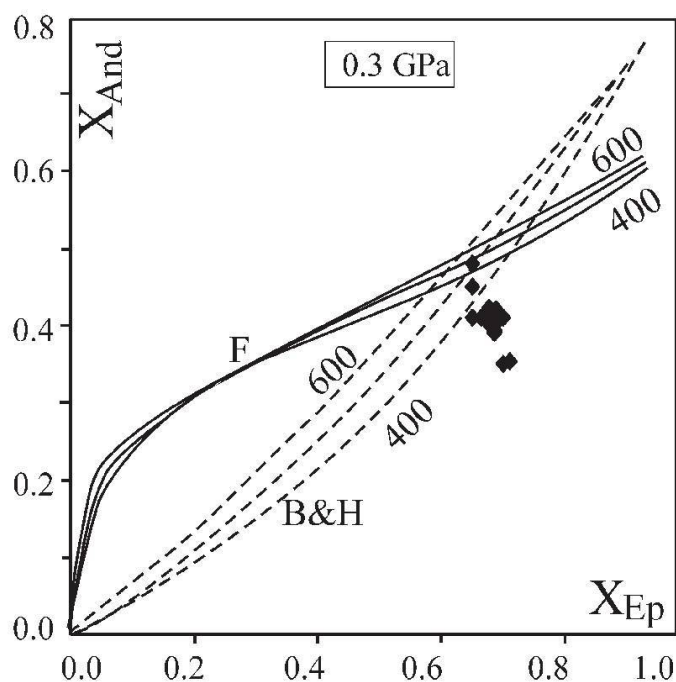
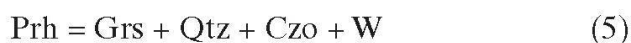


Fig. 8 Isotherms of the Al-Fe³⁺ distribution between coexisting epidote and grandite for the 400–600 °C temperature range at 0.3 GPa (B&H—Bird and Helgeson, 1980; F—Fehr, 1992). Diamonds represent data from this study.

timates are based on the methods developed by Holland and Blundy (1994), Anderson and Smith (1995). The pressure conditions calculated for sample MHV 564 range between 0.51–0.53 GPa at 703–734 °C.

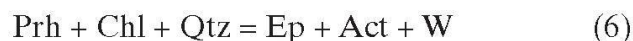
The stability field of grandite shows a wide temperature range (Meagher, 1980), but the presence of prehnite and Fe-rich epidote, assumed to be in equilibrium, suggest temperature < 400 °C (Cho and Liou, 1987). According to Kitamura (1975), Heuss-Assbichler and Fehr (1997), the partitioning of Al and Fe in epidote and grandite points to temperature dependence of the exchange reaction of $\text{Adr} + \text{Czo} = \text{Grs} + \text{Ep}$. Bird and Helgeson (1980) and Fehr (1992) developed an isobaric X_{Ep} vs. X_{And} diagram for coexisting epidote and grandite for the temperature range 400–600 °C at 0.3 GPa pressure (Fig. 8). Isotherms of both calculations fit well for X_{Ep} ca 0.7, which is the case of grandite-epidote from the Malá Fatra Mts. All analyses have $X_{\text{Adr}} < 0.5$, and excepting two analyses, they indicate temperature lower than 400 °C. Temperatures of 360–380 °C at 0.1–0.25 GPa (Fig. 9) are obtained for the reaction



calculated using the TWEEQ program (Berman, 1996; database JAN92) in the CASH system. The used activity models other than garnet and amphibole are listed in Table 7. Since the replace-

ment textures between individual Ca-Al silicates are rare, and all three Ca-Al silicates may occur within a single biotite pseudomorph, the temperature-dependent reaction between phases were probably too sluggish to proceed noticeably.

Temperature of ca 360 °C yielded the actinolite rimming edenite by the equilibrium reaction



which defines the upper temperature boundary of prehnite-actinolite facies in the CMASH system. Based on experimental data in the CO₂-free CMASH system (Cho and Liou, 1987), this reaction with two other boundary reactions between prehnite-pumpellyite and greenschist facies form an invariant point at 340 °C and 0.22 GPa. With increasing X_{CO_2} and $X_{\text{Fe}^{3+}}$, the invariant point shifts to lower pressures and temperatures. In our case, calcite is only an accessory phase in the studied rocks and probably has negligible effect on the reaction position.

Minerals clearly formed by the metamorphic overprint in the Malá Fatra rocks are: (1) zeolite forming drusy veins in tectonic zones, (2) white mica and epidote occurring in shear cracks, (3) adularia and calcite forming veinlets that cross cut other matrix minerals, including undulating quartz, in the granodiorite and tonalite. Compositional zoning of pumpellyite (increase of Mg and Al towards the rim) and its formation after prehnite

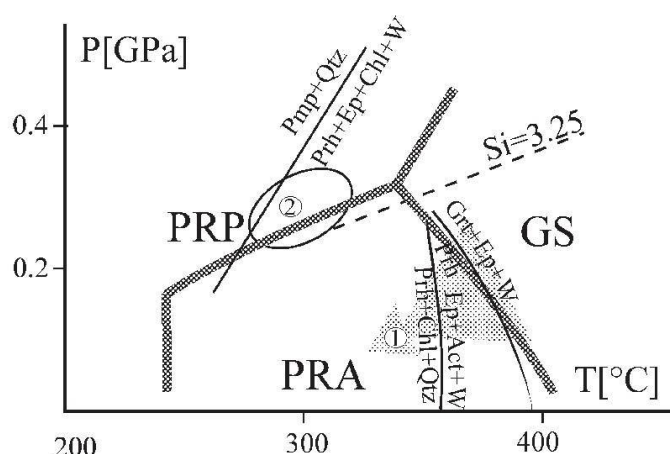


Fig. 9 P-T diagram showing the boundary reactions among prehnite-actinolite (PRA), prehnite-pumpellyite (PRP) and greenschist facies (GS) (after Cho and Liou, 1987). The Si isopleth for phengite is after Massonne and Schreyer (1987). The equilibrium reaction prehnite = grandite + epidote + H₂O was calculated in the CMASH system using the TWEEQ (Berman, 1996). Numbers in circles indicate inferred P-T conditions for post-magmatic alteration (1) and Alpine metamorphic overprint (2) in the Malá Fatra granodiorite and tonalite.

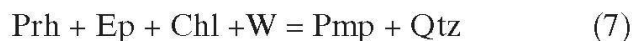
Table 7 Activity model and calculated activities used.

Phase	Structural formula	Activity	Ref.	Model activity
Prehnite (Prh)	$\text{Ca}_2\text{Al}_2\text{Si}_3\text{O}_{10}(\text{OH})_2$	X_{Al}	2	0.83*, 0.90**
Clinozoisite (Czo)	$\text{Ca}_2\text{Al}_3\text{Si}_3\text{O}_{12}(\text{OH})$	X_{Al}	1	0.70*, 0.72**
Chlorite (Clin)	$\text{Mg}_5\text{Al}_2[\text{Si}_3\text{O}_{10}](\text{OH})_8$	$0.7(X_{\text{Mg}})^5$	1	0.07*, 0.07**
Pumpellyite (Pmp)	$\text{Ca}_4\text{MgAl}_5\text{Si}_6\text{O}_{21}(\text{OH})_7$	$4X_{\text{Mg}}^{\text{M2}}X_{\text{Al}}^{\text{M2}}$	1	0.71**
Amphibole (Tr)	$\text{Ca}_2\text{Mg}_5\text{Si}_8\text{O}_{22}(\text{OH})_2$	$(X_{\text{Ca}}^{\text{M4}})^2(X_{\text{Mg}})^5(X_{\text{Si}}^{\text{T}})^8$	1	0.13*

References: (1) Evans (1990), (2) Bird and Helgeson (1980).

* and ** indicate activity models used in the post-magmatic and metamorphic reactions, respectively.

nite also suggest metamorphic origin of pumpellyite. All these minerals (Table 2) are indicative for very low-temperature deformation processes in the Malá Fatra Mts. Formation of pumpellyite after prehnite suggests transition from prehnite-actinolite to prehnite-pumpellyite facies that based, on the facies boundaries (Cho and Liou, 1987), indicates pressure of ca. 0.3 GPa at 300 °C. Temperature higher than 300 °C can be assumed by the lack of zeolite as equilibrium phase with prehnite or with pumpellyite. The equilibrium reaction



indicates a pressure of ca 0.4 GPa at 300 °C. If the phengite barometry of Massonne and Schreyer (1978) is valid for post-magmatic muscovite + K-feldspar, formed by replacement of biotite at $T < 400$ °C, then the pressure of ca. 0.3 GPa at 350 °C can be derived from the isopleth of $\text{Si} = 3.29$ a.f.u. However, this pressure is subject to a considerable uncertainty due to possible Fe^{3+} content in phengite.

5. Conclusions

The textural relations in granitic rocks from the Malá Fatra Mts indicate that Ti-bearing grandite garnet–epidote–prehnite and prehnite–epidote–actinolite–chlorite assemblages originated during post-magmatic hydrothermal alteration. The mass balance calculations among reacting and producing minerals suggest addition of fluids. Correlation between major elements in F- and Ti-bearing grandite indicates an exchange of $^{\text{VI}}\text{Ti}^{\text{IV}}\text{Fe}^{3+}\text{IV}\text{Si}_1^{\text{VI}}\text{Al}_1$ to andradite and grossularite for schorlomite. Equilibrium conditions calculated for coexisting garnet, epidote and prehnite were 360 °C at $P < 0.2$ GPa and for actinolite–epidote–chlorite ca. 380 °C. Considering P–T results of amphibole-plagioclase thermobarometry, the cooling of tonalite and granodiorite from their crystallization

to post-magmatic alteration and grandite formation took place by decreasing pressure and temperature from 703 °C/0.51 GPa to 360–380 °C/0.2 GPa.

The very low-grade metamorphic overprint, which led to mylonitization and ductile deformation of granitic rocks, probably related to Cretaceous tectonometamorphic processes, resulted in thrusting in the Western Carpathians units. Minerals formed during this event are pumpellyite replacing prehnite, epidote, phengite, chlorite and albite, thus indicating very low-grade P–T conditions of ca 0.3 GPa at 300 °C.

Acknowledgements

This work was supported by Scientific Grant Agency of the Slovak Republic through the project 1/8071/01. The manuscript was improved by thoughtful comments of J. K. Russell and of an anonymous reviewer.

References

- Anderson, J.L. (1996): Status of thermobarometry in granitic batholiths. *Transactions of the Royal Society of Edinburgh*, **87**, 125–138.
- Anderson, J.L. and Smith, D.R. (1995): The effect of temperature and oxygen fugacity on Al-in-hornblende barometry. *Am. Mineral.*, **80**, 549–59.
- Armbruster, T., Birrer, J., Libowitzky, E. and Beran, A. (1998): Crystal chemistry of Ti-bearing andradites. *Eur. J. Mineral.*, **10**, 907–921.
- Bagdasaryan, G.P., Gukasyan, R.Kh., Cambel, B., Kamenický, L. and Macek, J. (1992): Granitoids of the Malá Fatra and Vel'ká Fatra Mts.: Rb/Sr isochron geochronology (Western Carpathians). *Geol. Carpathica*, **43**, 21–25.
- Berman, R.G. (1996): TWEEQU (version 202), Thermobarometry with estimation of equilibration state <http://www.gis.nrcan.gc.ca/twq.html>
- Bird, D.K. and Helgeson, H.C. (1980): Chemical interaction of aqueous solutions with epidote-feldspar on mineral assemblages in geological systems. I. Thermodynamic analysis of phase relations in the system $\text{CaO-FeO-Fe}_2\text{O}_3\text{-Al}_2\text{O}_3\text{-SiO}_2\text{-H}_2\text{O-CO}_2$. *Am. J. Sci.*, **281**, 576–614.
- Broška, I., Diková, Z.P., Čelková, A. and Mokkov, A.V. (1992): Dusky apatite from the Variscan Granitoids of the Western Carpathians. *Geol. Carpathica*, **43**, 195–198.

- Broska, I., Petrík, I. and Benko, P. (1997): Petrology of the Malá Fatra granitoid rocks (Western Carpathians, Slovakia). *Geol. Carpathica*, **48**, 27–37.
- Holland, T. and Blundy, J. (1994): Non-ideal interactions in calcic amphiboles and their bearing on amphibole-plagioclase thermometry. *Contrib. Mineral. Petrol.*, **116**, 433–47.
- Cho, M. and Liou, J.G. (1987): Prehnite-Pumpellyite to Greenschist Facies Transition in the Karmutsen Metabasites, Vancouver Island, B.C. *J. Petrol.*, **28**, 417–443.
- Coombs, D.S., Kawachi, Y., Houghton, B.F., Hyden, G., Pringle, I.J. and Williams, J.G. (1977): Andradite and andradite-grossularite solid solutions in very low-grade regionally metamorphosed rocks in Southern New Zealand. *Contrib. Mineral. Petrol.*, **63**, 229–246.
- Evans, B.W. (1990): Phase relations of epidote-blue-schists. *Lithos*, **25**, 3–23.
- Fehr, K.T. (1992): Petrogenetische Teil-Netze für Nieder-temperatur-Hochdruck Metamorphite im System Ca-Al-Fe³⁺-Ti-Si-O-H. Habilitationsschrift, Fakultät für Geowissenschaften, Ludwig-Maximilians-Universität München, 211 pp.
- Freiberger, R., Hecht, L. and Cuney, M. (2001): Secondary Ca-Al silicates in plutonic rocks: Implication for their cooling history. *Contrib. Mineral. Petrol.*, **141**, 415–429.
- Henmi, Ch., Kusachi, I. and Henmi, K. (1995): Morimotoite, Ca₃TiFe²⁺Si₃O₁₂, a new titanian garnet from Fuka, Okayama Prefecture, Japan. *Mineral. Mag.*, **59**, 115–120.
- Heuss-Assbichler, S. and Fehr, K.T. (1997): Intercrystalline exchange of Al and Fe³⁺ between grossularite-andradite and clinozoisite-epidote solid solutions. *N. Jb. Miner. Abh.*, **172**, 69–100.
- Howie, R.A. and Woolley, A.R. (1968): The role of titanium and the effect of TiO₂ on the cell-size, refractive index, and specific gravity in the andradite-melanite-schorlomite series. *Mineral. Mag.*, **36**, 775–790.
- Janák, M. and Lupták, B. (1997): Pressure-temperature conditions of high-grade metamorphism and migmatization in the Malá Fatra crystalline complex. *Geol. Carpathica*, **48**, 455–488.
- Kamenecý, L., Macek, J. and Krštin, J. (1987): Contribution to petrography and geochemistry of granitoids in the Malá Fatra. *Mineralia Slov.*, **19**, 311–324.
- Kitamura, K. (1975): Al-Fe partitioning between garnet and epidote from the contact metasomatic copper deposits of the Chichibu Mine, Japan. *Econ. Geol.*, **70**, 725–738.
- Kühberger, A., Fehr, T., Huckenholz, H.G. and Amthauer, G. (1989): Crystal chemistry of a natural schorlomite and Ti-andradites synthesized at different oxygen fugacities. *Phys. Chem. Minerals*, **16**, 734–740.
- Labotka, T.C. (1995): Evidence for immiscibility in Ti-rich garnet in a calc-silicate hornfels from northeastern Minnesota. *Am. Mineral.*, **80**, 1026–1030.
- Lager, G., Armbruster, T., Rotella, F.J. and Rossman, G.R. (1989): OH substitution in garnets: X-ray and neutron diffraction, infrared, and geometric modeling studies. *Am. Mineral.*, **74**, 840–851.
- Leake, B.E. (1998): Widespread secondary Ca garnet and other silicates in the Galway granite and its satellite plutons caused by fluid movements, western Ireland. *Mineral. Mag.*, **62**, 381–386.
- Massonne H.J. and Schreyer, W. (1987): Phengite geobarometry based on the limiting assemblage with K-feldspar, phlogopite, and quartz. *Contrib. Mineral. Petrol.*, **96**, 212–224.
- Meagher, E.P. (1980): Silicate garnet. In: P.H. Ribbe (ed.): *Orthosilicates. Rev. Min.*, **5**, 28–66.
- Petrík, I., Broska, I. and Uher, P. (1994): Evolution of the Western Carpathian granite magmatism: Age, source rock, geotectonic setting and relation to the Variscan structure. *Geol. Carpathica*, **45**, 283–291.
- Russell, J.K., Dipple, G.M., Lang, J.R. and Lueck, B. (1999): Major-element discrimination of titanian andradite from magmatic and hydrothermal environments: an example from the Canadian Cordillera. *Eur. J. Mineral.*, **11**, 919–935.
- Tulloch, A.J. (1979): Secondary Ca-Al silicates as low-grade alteration products of granitoid biotite. *Contrib. Mineral. Petrol.*, **69**, 105–117.

Received 15 January 2002

Accepted in revised form 20 January 2003

Editorial handling: M. Engi